Parametric Simulation of PZT Diameter to Hole Ratio for Optimized Membrane Displacement

Arpys Arevalo*[1], David Conchouso[1], David Castro[1], and Ian G. Foulds[1,2]
[1]Computer, Electrical and Mathematical Sciences and Engineering (CEMSE), King Abdullah University of Science and Technology (KAUST), [2]The University of British Columbia (UBC), School of Engineering, Okanagan Campus.
*Corresponding author: 4700 KAUST, Kingdom of Saudi Arabia, arpys.arevalo@kaust.edu.sa

Abstract: In this paper, the parametric simulation of an acoustic transducer is presented. The modeling and analysis in COMSOL Multiphysics 5.0, shows the optimal configuration for the largest displacement of the membrane with the proposed material layers used. The Piezoelectric module was used to simulate the deflection of the membrane with an applied voltage. For this work, we varied the size of the piezoelectric material tri-layer (Pt/PZT/Pt) diameter and the hole where the membrane is clamped. The results show the optimal parameter to be used as the ratio between the PZT diameter and the total diameter of the membrane.

Keywords: acoustic transducer, PZT, MEMS, polyimide, ultrasonic transducer.

1. Introduction

Electronic systems have been continuously growing to a point that they play an important role in an average user. The demand of quality in the electronics industry products, requires the development of new components with better characteristics [1, 2]. Devices such as micro-speakers, microphones, accelerometers, gyroscopes, humidity sensors, lenses, cameras, amongst others, need better characteristics to keep up with the demand for quality.

An interesting gap to improve audio technology exists in one of the oldest components, the acoustic transducer. To improve the performance of the sound reproduction, we could potentially eliminate components that introduce noise when digital signals are converted to analog signals. The latter process usually occurs when reproducing sound in commercial loudspeaker drivers. One of the approaches we could take in order to tackle this problem, is the development of a system that can directly communicate from the digital audio signal source to a digital acoustic transducer, without the need to use a Digital-to-Analog converter (DAC). Such a system can be achieved with the concept of "Digital Sound Reconstruction" (DSR). The DSR concept can be implemented with a Digital Transducer Array Loudspeaker (DTAL) that was first proposed by Huang et al. in [3]. The device can be used to reproduce binary pulses that can be added together to reconstruct the analog audio signal. Actual problems or deficiencies associated with the current acoustic transducer, such as: frequency response and linearity, can be attenuated with this approach [4–6]. The DTAL can be organized by sets of transducers that are grouped in association with a bit-number. This configuration is refereed as "binary weighted group" [7]. For example, a 3-bit micro-speaker would have three sets of acoustic transducers, each group would have 2^n transducers (where n is the bit number). The most significant bit (MSB), would have 4 transducers (2^2 transducers). The second set would have 2 transducers (2^1 transducers), and the least significant bit (LSB) would have 1 transducer (2^0 transducers).

The DTAL device operates as follows: when a lower pressure is needed, fewer transducers are activated and when higher pressure is needed, more transducers are used. Each transducer contributes to a small pressure change in the system, which is a contribution of the total sound pressure change generated by the entire device.

The response time of an individual element only depends on the digital clock that synchronizes the audio reconstruction process. Therefore, each individual device is independent of the re-

constructed frequency and this enables the reconstruction of a wide range of frequencies. As a result, each membrane is not required to operate in a specific frequency range, in contrast to the current design rules of loudspeakers.

In this work, we use a piezoelectric material as the driving mechanism of our membrane, and polyimide as the structural material. Polyimide is a very attractive polymer for MEMS fabrication due to its low coefficient of thermal expansion, low film stress, lower cost than metals and semiconductors and high temperature stability compared to other polymers [8–10]. Polyimide has been previously used in the microelectronics industry for module packaging, flexible circuits and as a dielectric for multi-level interconnection technology [11, 12]. Recently, the polymer has been widely used as an elastic flexible substrate for polymerMEMS [13–15] and also as structural material for several devices [8, 13–27], which shows the extent of applications of the material.

Previously, the feasibility of such structure was reported [28, 29], but the performance was not as expected. Due to the low performance, we attempted to optimize the design of the membrane. We used Lead Zirconate Titanate (PZT) as the piezoelectric material with a bottom and top electrode using platinum (Pt), and a layer of polyimide as part of the structural material of the bimorph actuator.

2. Computational Methods

The interaction of the mechanics and the electrical fields of the studied structure is called piezoelectricity. The interactions are modeled as a coupling of the linear elasticity equations and charge relaxation time equations, using electric constants. Piezoelectricity can be described mathematically using the material's constitutive equations [**?**, 30, 31]. Piezoelectric materials become electrically polarized when they are subject to a strain. In a microscopic perspective, the atoms displacement when the solid is deformed causes electric dipoles within the material. In some cases, the crystal structures can give an average macroscopic dipole moment or electric polarization. This effect is known as the direct piezoelectric effect. Also its reciprocal exist, the converse piezoelectric effect, in which the solid contracts or expands when an electric field is applied.

The constitutive relation between the strain and the electric field in a piezoelectric material is shown below (strain-charge form):

$$\begin{aligned} \mathbf{S} &= s_E \mathbf{T} + d^T \mathbf{E} \\ \mathbf{D} &= d\mathbf{T} + \varepsilon_T \mathbf{E} \end{aligned} \tag{1}$$

Where, $\mathbf{S}$ is the strain, $\mathbf{T}$ is the stress, $\mathbf{E}$ is the electric field, and $\mathbf{D}$ is the electric displacement field. The materials parameters s_E, d and ε_T, correspond to the material compliance, the coupling properties and the permittivity of the material. These parameters are tensors of rank 4, 3 and 2 respectively. However they can be represented as matrices within an abbreviated subscript notation, as it is more convenient to handle. In COMSOL Multiphysics, the Piezoelectric Devices interface uses the Voigt notation, which is standard in the literature of piezoelectricity but differs from the defaults used in the Solid Mechanics interface. The latter equation (1) can be expressed in the stress-charge constitutive form, which relates the material stresses to the electric field:

$$\begin{aligned} \mathbf{T} &= c_E \mathbf{S} - e^T \mathbf{E} \\ \mathbf{D} &= d\mathbf{S} + \varepsilon_S \mathbf{E} \end{aligned} \tag{2}$$

The stress-charge form is usually used in the finite element method due to the useful match to the PDEs of Gauss' law (electric charge) and the Navier's equation (mechanical stress) [**?**]. Usually most material's properties are given in the strain-charge form. The material properties, c_E, e and ε_T are related to the parameters s_E, d and ε_T, and can be transformed between each other by the conversion equations shown below:

$$\begin{aligned} c_E &= s_E^{-1} \\ e &= d s_E^{-1} \\ \varepsilon_s &= \varepsilon_0 \varepsilon_{rT} - d s_E^{-1} d^T \end{aligned} \tag{3}$$

2.1 Governing Equations

The Piezoelectric equations used in COMSOL, combine the momentum equation,

$$\rho_0 \frac{\delta^2 \mathbf{u}}{\delta t^2} = \nabla_X (FS) + \mathbf{F}_V \tag{4}$$

with the charge conservation equation of Electrostatics,

$$\nabla \cdot \mathbf{D} = \rho_V \tag{5}$$

where the ρ_V is the electric charge concentration. The electric field is computed from the electric potential V as:

$$\mathbf{E} = -\nabla V \tag{6}$$

In both Equations (4) and (5), the constitutive relations of Equation (3) are used, which makes the resulting system of equations closed. The dependent variables are the structural displacement vector **u** and the electric potential V [**?**].

3. Design and Simulation Setup

The components of the piezoelectric membrane are: a 300nm platinum (Pt) bottom electrode, a 250nm piezoelectric layer (PZT), a 300nm Pt top electrode and a 3μm thick polyimide structural layer, to complete the bimorph membrane. In Fig. 1, the first version of our membrane is shown.

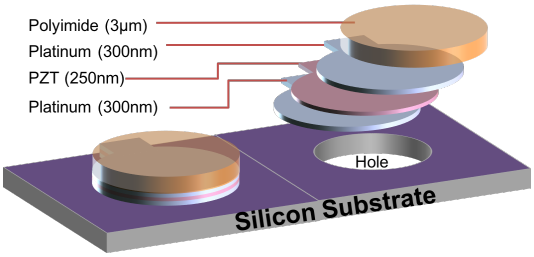

Figure 1: (Left) Isometric view of a membrane on silicon substrate (Right) Conceptual exploded view of the first design of the micro-membrane.

As it can be seen in the image, the piezoelectric actuator dimensions are larger than the hole area. This is the parameter that needs to be optimized, for a larger displacement of the membrane. In our simulation, we used the Piezoelectric module, whereby the structure was setup in a 2D environment. The structure was simulated as a cantilever, which is clamped from both sides, as shown in Fig. 2.

For the mechanical constraints the six vertical boundaries (edges) to each side of the structure was set to be fixed. All the other boundaries were set to be free. For the AC/DC interface the bottom

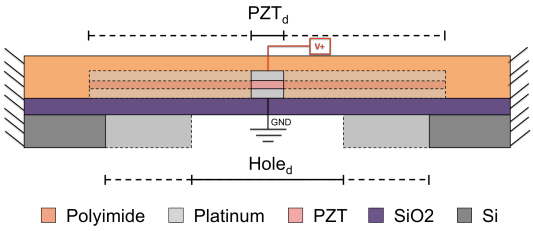

Figure 2: Schematic of the cross-secional view of the piezoelecric membrane.

electrode was set to be the ground, and the top electrode was set to be a Terminal with a potential of 10V.

A stationary study was selected and a parametric sweep was setup, to be able to change the geometry for different dimensions of the actuator. The PZT diameter dimension (shown in Fig. 2) will be constrained proportionally to the ratio "a", as shown below in Equation 7.

$$PZT_d = a * Hole_d \tag{7}$$

4. Results

The first version of the fabricated devices did not meet the expected performance, even though the transducers were able to reproduce sound waves. From the COMSOL simulation results, we were able to see that the original design was out of the optimal range parameters for a larger membrane displacement, see Fig. 3 and 4.

As seen above, the original design was really out of range for large membrane displacement. The range of displacement was in the range of hundreds of pico-meters. In Fig. 3, a 3D view produced from a revolution of the results is shown.

Due to these results, we were able to modify the device accordingly. In Fig. 5, a modified version of the membrane is shown. Where the desired PZT/Hole ratio "a" should be between 0.8 to 0.9, i.e. the Pt/PZT/Pt layers must have a diameter between $80\% - 90\%$ of the hole diameter area.

As seen in the conceptual view of Fig. 5, the piezoelectric stack has 4 arms. This arms will be the interconnection with the next element in the device array.

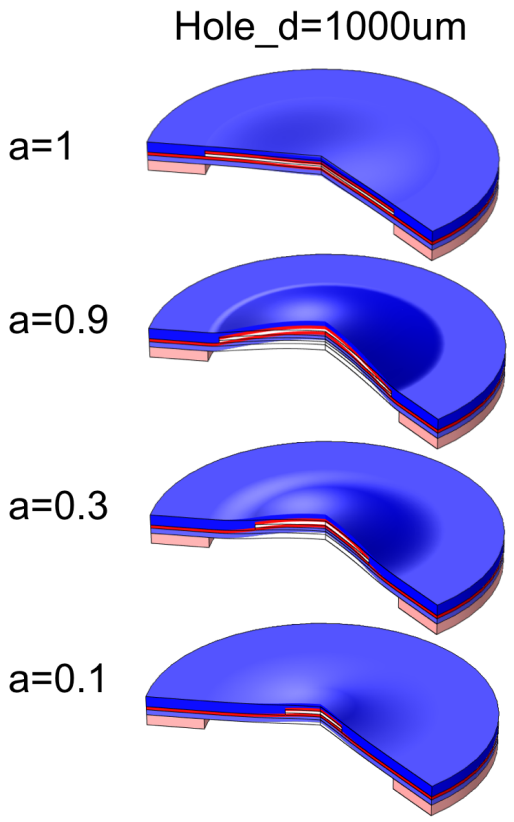

Figure 3: 3D representation from a partial revolution of the simulation results, showing the deformation of the membrane and the internal layers (colors depict the different materials in the structure).

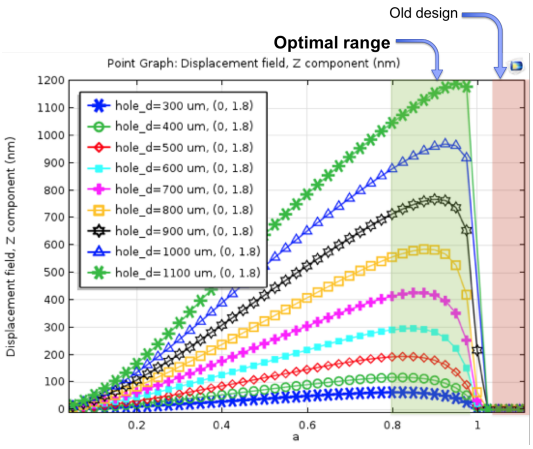

Figure 4: Displacement vs Diameter to Hole Ratio of the acoustic transducer.

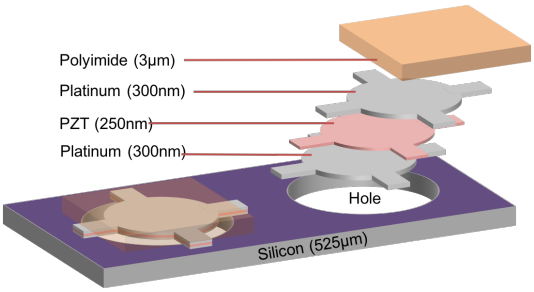

Figure 5: Conceptual view of the new membrane design for the Pt/PZT/Pt layer stack for optimized membrane displacement.

5. Conclusions

After analyzing the simulation results, we noticed that the original parameter designs were not optimal. New designs were developed to get a better performance of the array of actuators. The next steps in the project include simulations of the acoustic energy generated by the acoustic transducers. We have fabricated and diced the chips from a four inch silicon wafer using our in-house dicing method [32]. An interesting characteristic that we will also consider, is the directivity of the beam forming pattern, which is an inherit characteristic of the final transducer array.

The device will work as a directional loudspeaker, either using the Digital Sound Reconstruction concept or by signal modulation using an ultrasonic signal, which contains the audible signal. This characteristic, has great potential for a wide range of applications for our MEMS microloudspeaker, such as: separate multi-user intensity and signal control of the audio source, private audio, medicine, underwater communication, to name but a few.

6. References

1. J P Rojas, A Arevalo, I G Foulds, and M M Hussain. Design and characterization of ultra-stretchable monolithic silicon fabric. *Applied Physics Letters*, **105**(15):154101, (2014).

2. J P Rojas, Hussain A M, A Arevalo, I G Foulds, Sevilla GAT, JM Nassar, and M M Hussain. Transformational electronics are

now reconfiguring. *SPIE Defense+ Security*, **9467**:946709–946709–7, (2015).

3. Yaxiong Huang, Simon C Busbridge, and Denshinder S Gill. Directivity and Distortion in Digital Transducer Array Loudspeaker. *Journal of the Audio Engineering Society*, (2000).

4. B.M Diamond, J.J. Jr Neumann, and K.J Gabriel. Digital sound reconstruction using arrays of CMOS-MEMS microspeakers. In *Micro Electro Mechanical Systems, 2002. The Fifteenth IEEE International Conference on*, pages 292–295, (2002).

5. Hyejin Kim, Sungq Lee, Sangkyun Lee, and Kangho Park. A piezoelectric microspeaker with a high-quality PMN-PT single-crystal membrane. *Journal of Korean Physical Society*, **54**:930, (2009).

6. Fotios Kontomichos, John Mourjopoulos, and Nicolas-Alexander Tatlas. Alternative Encoding Techniques for Digital Loudspeaker Arrays. *Journal of the Audio Engineering Society*, (2007).

7. A Arevalo, D Conchouso, D Castro, N Jaber, M I Younis, and I G Foulds. Towards a Digital Sound Reconstruction MEMS Device: Characterization of a Single PZT Based Piezoelectric Actuator. In *10th IEEE International Conference on Nano/Micro Engineered and Molecular Systems NEMS2015*, Xia'an (2015).

8. A Arevalo, E Byas, D Conchouso, D Castro, S Ilyas, and I G Foulds. A Versatile Multi-User Polyimide Surface Micromachining Process for MEMS Applications. In *10th IEEE International Conference on Nano/Micro Engineered and Molecular Systems NEMS2015*, Xia'an (2015).

9. A A A Carreno, D Conchouso, A Zaher, I Foulds, and J Kosel. Simulation of a Low Frequency Z-Axis SU-8 Accelerometer in CoventorWare and MEMS+. In *Computer Modelling and Simulation (UKSim), 2013 UKSim 15th International Conference on*, pages 792–797, (2013).

10. D Conchouso, A Arevalo, D Castro, E Rawashdeh, M Valencia, A Zaher, J Kosel, and I Foulds. Simulation of SU-8 Frequency-Driven Scratch Drive Actuators. In *Computer Modelling and Simulation (UKSim), 2013 UKSim 15th International Conference on*, pages 803–808, (2013).

11. A Bruno Frazier. Recent applications of polyimide to micromachining technology. *Industrial Electronics, IEEE Transactions on*, **42**(5):442–448, (1995).

12. A B Frazier. Uses of polyimide for micromachining applications. In *Industrial Electronics, Control and Instrumentation, 1994. IECON '94., 20th International Conference on*, pages 1483–1487, (1994).

13. S.Y. Xiao, L.F. Che, X.X. Li, and Y.L. Wang. A novel fabrication process of {MEMS} devices on polyimide flexible substrates. *Microelectronic Engineering*, **85**(2):452 – 457, (2008).

14. Steve Tung, Scott R Witherspoon, Larry A Roe, Al Silano, David P Maynard, and Ned Ferraro. A mems-based flexible sensor and actuator system for space inflatable structures. *Smart Materials and Structures*, **10**(6):1230, (2001).

15. J. Courbat, M.D. Canonica, D. Briand, N.F. de Rooij, Damien Teyssieux, Laurent Thiery, and Bernard Cretin. Thermal simulation and characterization for the design of ultra-low power micro-hotplates on flexible substrate. In *Sensors, 2008 IEEE*, pages 74–77 (2008).

16. A Arevalo, E Byas, and I G Foulds. μHeater on a Buckled Cantilever Plate for Gas Sensor Applications. *2012 COMSOL Conference, Milan, Italy*, (2012).

17. A Arevalo, D Conchouso, and I G Fould. Optimized Cantilever-to-Anchor Configuration of Buckled Cantilever Plate Structures for Transducer Applications. *2012 COMSOL Conference, Milan, Italy*, (2012).

18. A Arevalo, S Ilyas, D Conchouso, and I G Foulds. Simulation of a Polyimide Based Micromirror. *2014 COMSOL Conference*, (2014).

19. A Arevalo and I G Foulds. Polyimide Thermal Micro Actuator. *2014 COMSOL Conference, Cambridge, England*, (2014).

20. S Ilyas, A Ramini, A Arevalo, and M I Younis. An Experimental and Theoretical Investigation of a Micromirror Under Mixed-Frequency Excitation. *Journal of Microelectromechanical Systems*, (2015).

21. D Conchouso, A Arevalo, D Castro, , and I G Foulds. Out-of-plane Platforms with Bidirectional Thermal Bimorph Actuation for Transducer Applications. In *10th IEEE International Conference on Nano/Micro Engineered and Molecular Systems NEMS2015*, Xia'an (2015).

22. Loïc Marnat, A Arevalo Carreno, D Conchouso, M Galicia Martinez, I Foulds, and Atif Shamim. New Movable Plate for Efficient Millimeter Wave Vertical on-Chip Antenna. *IEEE Transactions on Antennas and Propagation*, **61**(4):1608–1615, (2013).

23. A Alfadhel and Arpys Arevalo. Three-Axis Magnetic Field Induction Sensor Realized on Buckled Cantilever Plate. ... *IEEE Transactions on*, (2013).

24. D Castro, A Arevalo, E Rawashdeh, and N Dechev. Simulation of a Micro-Scale Out-of-plane Compliant Mechanism. In *2014 COMSOL Cambridge, England*, (2014).

25. A Arevalo, D Conchouso, D Castro, M Diaz, and I G Foulds. Out-of-plane buckled cantilever microstructures with adjustable angular positions using thermal bimorph actuation for transducer applications. *Micro and Nano Letters*, (2015).

26. A Arevalo, D Conchouso, E Rawashdeh, D Castro, and I G fould. Platform Isolation Using Out-of-Plane Compliant Mechanisms. In *2014 COMSOL Conference, Boston, USA* (2014).

27. N Jaber, A Ramini, A Carreno, and MI Younis. Higher Order Modes Excitation of Micro Clamped-Clamped Beams. *NANOTECH Dubai 2015*, (2015).

28. Arpys Arevalo and I G Foulds. Parametric Study of Polyimide–Lead Zirconate Titanate Thin Film Cantilivers for Transducer Applications. *COMSOL Rotterdam*, (2013).

29. A Arevalo and I G Foulds. MEMS Acoustic Pixel. *2014 COMSOL Conference, Cambridge, England*, (2014).

30. Prakruthi Hareesh, Isaac Misri, Shuang Yang, and Don L DeVoe. Transverse Interdigitated Electrode Actuation of Homogeneous Bulk PZT. *Journal of Microelectromechanical Systems*, **21**(6):1513–1518, ().

31. Y B Jeon, R Sood, J h Jeong, and S G Kim. MEMS power generator with transverse mode thin film PZT. *Sensors and Actuators A: Physical*, **122**(1):16–22 (2005).

32. Yiqiang Fan, Arpys Arevalo, Huawei Li, and Ian G Foulds. Low-cost silicon wafer dicing using a craft cutter. *Microsystem Technologies*, **21**(7):1–4, (2014).